

## NUMERICAL SIMULATION ON TYPICAL PARTS EROSION OF THE OIL PRESSURE PIPELINE

by

**Huanhuan WU, Xiaoyu LIANG\*, and Zhiqiang DENG**

College of Metrology & Measurement Engineering, China Jiliang University,  
Hangzhou, China

Original scientific paper  
DOI: 10.2298/TSCI1305349W

*Unscheduled shut-downs of oil pipeline caused by erosion have great negative influence on production efficiency of enterprises. In this article, a computational fluid dynamics software is applied to simulate flow in bend and sudden expansion pipe to analyze erosion distribution of inner wall under different conditions.*

**Keywords:** oil pipeline, erosion, bend, sudden expansion pipe, simulation

### Introduction

Oils are always output with sands during the oilfield development, and the growing of the sand content in the crude-oil may bring a lot of damage to the oil transportation system. A large number of studies [1-3] were carried out on the erosion problem of pipe. Huang *et al.* [4] summarized several kinds of erosion models for gas flows and liquid flows. Stack and Abdelrahman [5] evaluated the effects of particle concentration on the erosion-corrosion of the inner surfaces of 90° bend by computational fluid dynamics model. Brown [6] developed a 3-D CFD model to predict the motion of caustic liquor and bauxite particles through a tee-junction, and found that CFD techniques can be used effectively in industry erosion problems. Oka *et al.* [7] and Oka and Yoshida [8] discussed the effects of impact parameters in a predictive equation and the mechanical properties of materials directly associated with erosion damage.

In order to study the influence of pipeline structure on erosion distribution, in this article flow field simulation of bends with different cambers, different ratios of bending radius to diameter and sudden expansion pipes with different sudden expansion ratios are conducted to study the erosion distribution on pipes cause by the oil with 0.5% sand content.

### Geometric model

Models and meshes are built and divided by Gambit software. Figure 1 shows the geometry diagram of 90° bend. Figure 2 shows geometry diagram of sudden expansion pipe.

### Mathematical model

Fluid in pipe is satisfied with the continuity equation and momentum conservation equation. A standard  $k-\varepsilon$  turbulence model

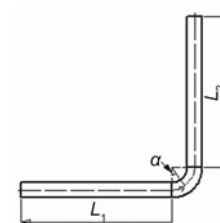


**Figure 1. Geometric model of 90° bend**

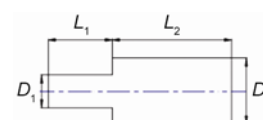


**Figure 2. Geometric model of sudden expansion pipe**

\* Corresponding author; e-mail: xyliang@cjlu.edu.cn

is selected with standard wall functions and zero roughness for its features of wide application scope, economic usefulness, and good accuracy. Discrete phase model (DPM) is used in this article. The control equations are dispersed by one-order upwind scheme and solved by SIMPLE arithmetic. Velocity inlet is selected as condition of entrance boundary. Outflow is selected as condition of exit boundary. No slip is selected as condition of wall boundary.

In this article, Hashish erosion model [9] is used and can be given by:

$$E = \frac{100}{2\sqrt{29}} r_p^3 \left( U_p \sqrt{\frac{\rho_p}{3\sigma R_f^{0.6}}} \right)^n \sin 2\alpha \sqrt{\sin \alpha} \quad (1)$$

where  $U_p$  is the particle velocity,  $\rho_p$  – the particle density with  $2650 \text{ kgm}^{-3}$ ,  $R_f$  – the roundness factor with 0.5,  $\sigma$  – the plastic flow stress with  $1.0\text{E}+09 \text{ Pa}$ ,  $r_p$  – the particle radius with  $2.5\text{E}-4 \text{ m}$ ,  $n$  – the velocity ratio exponent with 2.54, oil density is  $820.1 \text{ kgm}^{-3}$  with  $3 \text{ ms}^{-1}$  in inlet velocity, oil dynamic viscosity is  $2.651\text{E}-3 \text{ Pa}\cdot\text{s}$ , sand content of oil is 0.5%, and the diameter of pipe is 0.0508 m.

### Computational simulations of bend

#### *Analysis of pressure and velocity in bend*

Figure 3 shows that pressure in pipe generally decreases along the flow direction. When directions of fluid in elbow are changed, fluid slings and extrudes to extrados under action of centrifugal force, which make the pressure on extrados larger than intrados. Due to inertia effect, the fluid that just leaves elbow will not immediately restore to original state in straight pipe.

Distribution of velocity is plotted in fig. 4, which shows that a high velocity zone is generated next to intrados of elbow and a low velocity zone is generated downstream of intrados. Secondary flow [10] is formed which is illustrated in fig. 5. On a cross-section of elbow, fluid starts from extrados, flows to intrados along the tangential direction of the circumference and backs to extrados through the center of the cross-section area. Secondary flow has an effect on distribution of erosion rate.

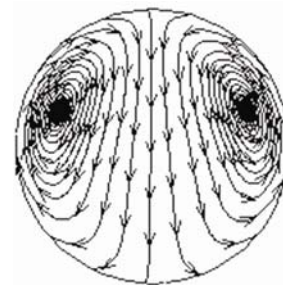
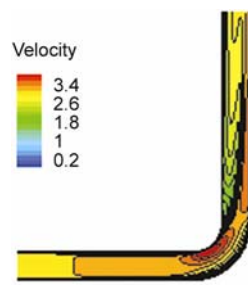
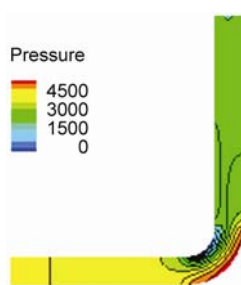


**Figure 3. Pressure distribution** **Figure 4. Velocity distribution** **Figure 5. Streamline on cross section**  
(for color image see journal website)

#### *Analysis of erosion distribution on bend*

Figure 6 shows distribution of particle impact angle and impact frequency on  $90^\circ$  bend with 1.5 in ratios of bending radius to diameter, and fig. 7(a) shows erosion distribution on intrados and extrados of  $90^\circ$  bend. Impact angle, impact frequency and erosion on straight pipe are much smaller than elbow since the flow direction of fluid in straight pipe is parallel to

the pipe axis which leads to less impact to pipe wall. On elbow, as the flow direction changes, fluid and particles impact the pipe wall and produce larger erosion. A small amount of erosion appears on elbow when  $\alpha = 20\text{-}30^\circ$  and grows with the increment of  $\alpha$  and reaches the maximum at  $\alpha = 80\text{-}90^\circ$ . The biggest impact frequency is mainly concentrated at  $\alpha = 80\text{-}90^\circ$ . The particle firstly dose curvilinear motion under the influence of bend and then impacts the wall, as a result, the erosion is mainly distributed in the second half of extrados. It is worth noting that erosion rate is infinitesimally small on intrados. Instead, larger erosion area appear on the left and right side of the straight pipe near elbow and surround to inner side of straight pipe. This part of erosion is mainly caused by the secondary flow. Although left the elbow, secondary flow still exists in a part of straight pipe near elbow. Thus particles impact wall at a certain angle under the influence of secondary flow and erosion produced on straight pipe near elbow.

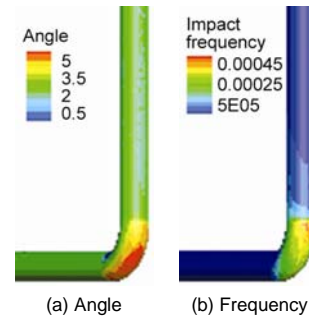


**Figure 6. Distribution of impact angle and impact frequency**  
(for color image see journal website)

According to fig. 7, erosions of the three kinds of bends are consistent at  $\alpha = 10\text{-}30^\circ$ , extrados of elbow is the main erosion area. Area and strength of erosion are greatly reduced, especially for the  $30^\circ$  bend. As well as  $90^\circ$  bend, the maximum erosion rate of both kinds of bends are distributing, respectively, at  $\alpha = 45^\circ$  and  $\alpha = 30^\circ$ . As camber decreases, intensity of secondary flow is reduced, which is the reason that erosion rate on straight pipe near export of elbow become disperse, and surrounds of inner side of pipe are less obvious than  $90^\circ$  elbow. Figure 8 shows erosion distribution of bends under different ratios of bending radius to diameter in 2, 3, 4, 5, 6, and 10, respectively. Erosion of elbow reduces successively because the greater of ratios make the flow of fluid in elbow more close to straight pipe. Meanwhile, erosion on straight pipe near export of elbow gradually disappears because secondary flow becomes weak. Erosion is mainly distributed on extrados of elbow at  $\alpha = 30\text{-}90^\circ$ .

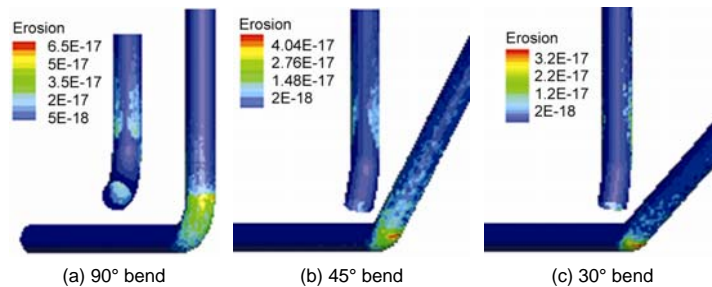


**Figure 7. Distribution of erosion under different cambers**  
(for color image see journal website)

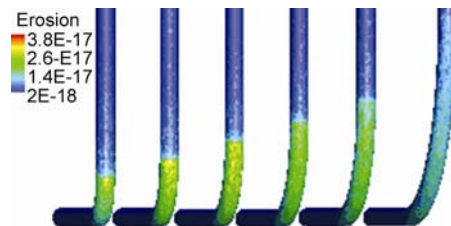


**Figure 8. Erosion under different ratios of bending radius to diameter**  
(for color image see journal website)

## Computational simulations of sudden expansion pipe

### Analysis of pressure and velocity in sudden expansion pipe

Figure 9 shows that pressure decreases gradually in small pipe and achieves the minimum value in diameter enlargement zone because of the increasing of local energy loss. The

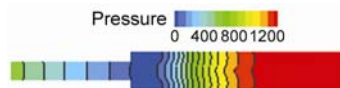


Figure 9. Pressure distribution

(for color image see journal website)



Figure 10. Velocity distribution

pressure in the second half of big pipe is bigger than the small pipe. According to fig. 10, the main stream still keeps large speed after leaving diameter enlargement

zone, and circumfluence and vortex generate between the corner of sudden expansion pipe and main stream. With fluid flow away from diameter enlargement zone, the eddy current effect reduces progressively to zero.

#### Analysis of erosion distribution on sudden expansion pipe

Figures 11 and 12 show the distributions of particle impact angle and impact frequency, respectively. The reason why zone B has bigger impact frequency is that flow separation phenomenon form in

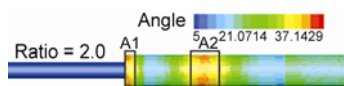


Figure 11. Distribution of impact angle

(for color image see journal website)

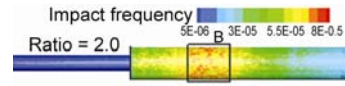
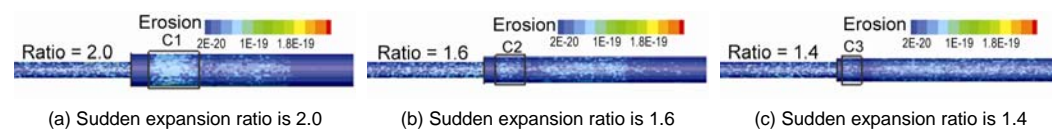


Figure 12. Distribution of impact frequency

pipe corresponding to zone B leads to a part of the fluid backflow and particles impact pipe wall with fluid simultaneously. Zone A1 and A2 both have big impact angle about 40-45°.

Sudden turn of directions of fluid in zone A1 and A2 could be the reason why impact angle there are biggest.

According to fig. 13(a), erosion distributes uniformly on small pipe. On big pipe erosion is mainly concentrated on zone C1 and the impact angle ranges from 17° to 35°. After zone C1, erosion rate decreases first, then increases slightly, and finally disperses. Erosion on zone between diameter enlargement zone and C1 is extremely small because the fluid velocity there is very small.



(a) Sudden expansion ratio is 2.0

(b) Sudden expansion ratio is 1.6

(c) Sudden expansion ratio is 1.4

Figure 13. Erosion under different sudden expansion ratios (for color image see journal website)

It can be seen from the analysis that although fluid velocity, impact angle and impact frequency have big influence on erosion rate, the pipe wall having the biggest velocity or the biggest impact frequency or the biggest impact angle does not mean it will have the biggest erosion rate. For example, zone C1 only has a minority of intersection with zone B and disjoint with A1, A2. Therefore, erosion is determined by the combined effects of velocity, impact angle and impact frequency.

Figure 13 shows erosion distribution under different sudden expansion ratios of 2.0, 1.6, and 1.4. For the sudden expansion pipe with 1.4 ratios, the erosion on whole pipeline is relatively uniform except the wall close to recirculation zone. When sudden expansion ratio increases to 1.6, erosion gradually become focused on zone C2. This situation becomes more obvious when ratio reach 2.0. In addition, with the ratios increasing, the range of erosion zone C1 is bigger than zone C2 and zone C3.

## Conclusions

A small amount of erosion appears on elbow at  $\alpha = 20\text{-}30^\circ$  and grows with the increment of  $\alpha$  and reaches the maximum at  $\alpha = 80\text{-}90^\circ$ . Area and strength of erosion are much reduced with the decrease of bend camber. With the decrease of ratios of bending radius to diameter, erosion rate reduces and mainly distributes on extrados of elbow at  $\alpha = 30\text{-}90^\circ$ .

For sudden expansion pipe, erosion is mainly concentrated on the wall that corresponding to re-circulation zone. With the decrease of sudden expansion ratios, erosion concentrated on the wall corresponding to recirculation zone becomes disperse well-proportioned on whole section of big pipe.

## Acknowledgment

This work was supported by National Special Fund for Quality Inspection Research in the Public Interest under Grant 201210026.

## Nomenclature

$E$  – volume erosion, [ $\text{m}^3$  per impact]  
 $n$  – velocity ratio exponent, [–]  
 $r_p$  – particle radius, [m]  
 $R_f$  – roundness factor for particle, [–]  
 $U_p$  – particle velocity, [ $\text{ms}^{-1}$ ]

### Greek symbols

$\alpha$  – particle impact angle, [ $^\circ$ ]  
 $\rho_p$  – particle density, [ $\text{kgm}^{-3}$ ]  
 $\sigma$  – plastic flow stress for target, [Pa]

## References

- [1] Shah, S. N., Jain, S., Coiled Tubing Erosion during Hydraulic Fracturing Slurry Flow, *Wear*, 264 (2008), 3, pp. 279-290
- [2] Wood, R. J. K., *et al.*, Comparison of Predicted and Experimental Erosion Estimates in Slurry Ducts, *Wear*, 256 (2004), 9, pp. 937-947
- [3] Njobuenwu, D., *et al.*, Modeling of Pipe Bend Erosion by Dilute Particle Suspensions, *Computers and Chemical Engineering*, 42 (2012), pp. 235-247
- [4] Huang, Y., *et al.*, Forecast and Prevention of Erosion in Elbow (in Chinese), *Petroleum Refinery Engineering*, 35 (2006), 2, pp. 33-36
- [5] Stack, M. M., Abdelrahman, S. M., A CFD Model of Particle Concentration Effects on Erosion- Corrosion of Fe in Aqueous Conditions, *Wear*, 273 (2011), 1, pp. 38-42
- [6] Brown, G. J., Erosion Prediction in Slurry Pipeline Tee-Junctions, *Applied Mathematical Modelling*, 26 (2006), pp. 2, 155-170
- [7] Oka, Y. I., *et al.*, Practical Estimation of Erosion Damage Caused by Solid Particle Impact, Part 1: Effects of Impact Parameters on a Predictive Equation, *Wear*, 259 (2005), 1, pp. 95-101
- [8] Oka, Y. I., Yoshida, T., Practical Estimation of Erosion Damage Caused by Solid Particle Impact, Part 2: Mechanical Properties of Materials Directly Associated with Erosion Damage, *Wear*, 259 (2005), 1, pp. 102-109
- [9] Wood, R. J. K., Jones, T. F., Investigations of Sand-Water Induced Erosive Wear of AISI 304L Stainless Steel Pipes by Pilot-Scale and Laboratory-Scale Testing, *Wear*, 255 (2003), 1, pp. 206-218
- [10] Sun, Y. Z., *et al.*, Numerical Study on Flow Characteristics of  $90^\circ$  Bend Pipe under Different Reynolds Number (in Chinese), *University of Shanghai for Science and Technology*, 32 (2010), 1, pp. 525-529